Information Entropy-Based Viewpoint Planning for 3-D Object Reconstruction

Y. F. Li, *Senior Member, IEEE,* and Z. G. Liu

Abstract—In this paper, we present an information entropy-based viewpoint-planning approach for reconstruction of freeform surfaces of three-dimensional objects. To achieve the reconstruction, the object is first sliced into a series of cross section curves, with each curve to be reconstructed by a closed B-spline curve. In the framework of Bayesian statistics, we propose an improved Bayesian information criterion (BIC) for determining the B-spline model complexity. Then, we analyze the uncertainty of the model using entropy as the measurement. Based on this analysis, we predict the information gain for each cross section curve for the next measurement. After predicting the information gain of each curve, we obtain the information change for all the B-spline models. This information gain is then mapped into the view space. The viewpoint that contains maximal information gain about the object is selected as the next best view. Experimental results show successful implementation of our view planning method for digitization and reconstruction of freeform objects.

Index Terms—B-spline, information entropy, 3-D reconstruction, uncertainty-driven, viewpoint planning.

I. INTRODUCTION

RECONSTRUCTING three-dimensional (3-D) object surfaces from 3-D data points is important to many applications such as reverse engineering, object recognition, inspection, computer graphics and medical imaging. Currently, a laser range finder/scanner [1] is widely used for 3-D surface data acquisition in industry. To increase the efficiency in the 3-D imaging, the use of pattern projections has been explored [2]. Portable 3-D imaging systems based on such a principle have been designed [3]. To plan the best viewpoints so that all the information about the object surface can be acquired in an optimal way, the next best view (NBV) problem has been studied in recent research. The problem of viewpoint planning [4] for digitalization of 3-D objects can be treated in different ways, depending on whether or not the object's geometry is known beforehand [5], [6]. For an unknown object, since the number of viewpoints and their viewing pose can not be determined prior to data acquisition, the 3-D reconstruction has to be carried out in an incremental way with iterative cycles of viewpoint planning, data acquisition, registration, and view integration.

Over the years, different NBV algorithms have been proposed in the literature. Connolly [7] used octree to represent object space. The regions that have been scanned were labeled as seen, regions between the sensor and surface as empty, and all other regions as unseen. A set of candidate viewpoints was enumerated with fixed increments around the object. The NBV was calculated based on evaluation of the visibility of each candidate viewpoint. This algorithm is computationally expensive and it does not incorporate the sensor geometry. Maver and Bajcsy [8] presented a solution to the NBV problem for a specific scanning setup consisting of an active optical range scanner and a turntable. Unseen regions of the objects were represented as polygons. Visibility constraints for the sensor to view the unseen region were computed from the polygon boundaries. However, this solution is limited to a particular sensor configuration. Pito [9] proposed an approach based on an intermediate position space representation of both sensor visibility constraints and unseen portions of the viewing volume. The NBV was determined as the sensor position that maximized the unseen portion of the object volume. This approach was demonstrated to have achieved automatic viewpoint-planning for a range sensor constrained to move on a cylindrical path around the object. Whaite and Ferrie [10] used superellipsoid model to represent the object and defined a shell of uncertainty. The NBV was selected at the sensor position where the uncertainty of the current model fitted to the partial data points is largest. This algorithm enables uncertainty-driven exploration of an object to build its model. However, superellipsoid cannot accurately represent objects with complex surface shapes. Furthermore, surface visibility constraints were not incorporated in the viewpoint-planning process. Reed and Allen [11] proposed a target-driven viewpoint-planning method. The volume model was used to represent the object by extrusion and intersection operation. The constraints, such as sensor imaging constraint, model occlusion constraint, and sensor placement constraint, were represented as solid modeling volumes and incorporated into the viewpoint planning. The algorithm involved expensive computation on the volume in the solid modeling and intersection operation. Scott [12] considered viewpoint planning as integer programming problem. Given a rough model of an unknown object, a sequential set of viewpoints was calculated to cover all surface patches of the object with the registration constraint. However, the object must be scanned before viewpoint planning to obtain the prior knowledge about unknown objects.

This paper presents an information entropy based viewpoint-planning method for the digitization and reconstruction of 3-D

Y. F. Li is with Department of Manufacturing Engineering and Engineering Management, City University of Hong Kong, Kowloon, Hong Kong (e-mail: meyfli@cityu.edu.hk).

Z. G. Liu was with the Department of Manufacturing Engineering and Engineering Management, City University of Hong Kong, Kowloon, Hong Kong. He is now with the National Key Laboratory of Manufacturing System Engineering, Xi'an Jiaotong University, Xi'an, China.
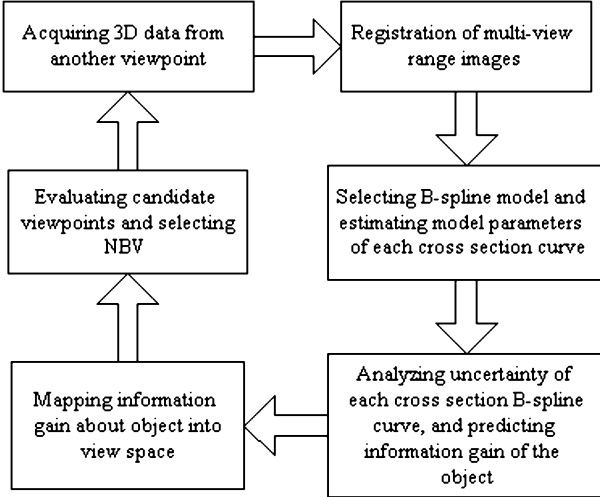
Fig. 1. Information entropy based viewpoint planning.

freeform object. The object is sliced into a set of cross section curves, and a closed B-spline curve is used to reconstruct each cross section curve by fitting to partial data points. An information criterion is developed for selecting the B-spline model structure. Based on the selected B-spline model, we use information entropy as the uncertainty measure of the B-spline model, and analyze the uncertainty of each B-spline cross section curve to predict the information gain for new measurements to be taken. As a result, we can obtain the prediction of the information gain about the object. The information gain is then mapped to the view space. The view that has the maximal information gain about the object is then selected as the NBV. The proposed information entropy based viewpoint-planning procedure is illustrated in Fig. 1.

Our work is original in the parameter estimation for the NBV problem. Different from Whaite's method [10], we analyze and reconstruct B-spline model in the framework of Bayesian statistics. The B-spline model is more powerful in describing objects than superellipsoids. In addition, we introduce the principle of model selection by which our proposed improved Bayesian information criterion (BIC) makes the B-spline model adaptable when newly acquired data are available. The rest of this paper is organized as follows. In Section II, we describe the reconstruction of cross section curves with closed B-splines and introduce the modified BIC for selecting the B-spline model structure. In Section III, we define the information entropy of B-spline model to analyze its uncertainty and predict information gain about an object. In Section IV, we evaluate the visibility of candidate viewpoints for selecting NBV. Finally, we present the experimental results in implementing the proposed method in Section V, followed by conclusions in Section VI.

II. B-SPLINE RECONSTRUCTION AND MODEL SELECTION

A. Why B-Spline?

For object surface reconstructions, the 3-D shape can be divided into a series of cross section curves, each representing the local geometrical feature of the object. These cross section curves can be described by a set of parametric equations. For reconstruction purposes using parametric equations, the most

common methods include spline function (e.g., B-spline) [13], implicit polynomial and superquadric (e.g., superellipsoid) [10]. Compared with implicit polynomial, and superquadric, B-spline has the following main advantages.

1) *Smoothness and continuity*, which allows a curve to consist of a concatenation of curve segments, yet be treated as a single unit.
2) *Built-in boundedness*, a property which is lacking in implicit or explicit polynomial representation whose zero set can shoot to infinity.
3) *Parameterized representation*, which decouples the x, y coordinates to be treated separately.

B. Closed B-Spline Curve Approximation

Let a closed cubic B-spline curve consist of $n + 1$ curve segments, defined by

$$\mathbf{p}(t) = \sum_{j=0}^{n+3} B_{j,4}(t) \cdot \mathbf{\Phi}_j \qquad (1)$$

where $\boldsymbol{p}(t) = [x(t), y(t)]$ is a point on the B-spline curve with location parameter t. $B_{j,4}(t)$ is the jth normalized cubic B-spline basis function defined over the following uniform knots vector:

$$[u_{-3}, u_{-2}, u_{-1}, u_0, \ldots, \ldots, u_{n+4}]$$
$$= [-3, -2, -1, 0, \ldots, n+4]. \quad (2)$$

The amplitude of $B_{j,4}(t)$ is in the range of (0.0, 1.0), and the support region of $B_{j,4}(t)$ is compact and nonzero for $t \in [u_j, u_{j+4}]$. $(\mathbf{\Phi}_j)_{j=0}^{n+3}$ are the cyclical control points which satisfy the following conditions:

$$\mathbf{\Phi}_{n+1} = \mathbf{\Phi}_0, \quad \mathbf{\Phi}_{n+2} = \mathbf{\Phi}_1, \quad \mathbf{\Phi}_{n+3} = \mathbf{\Phi}_2. \quad (3)$$

For a set of m data points $\boldsymbol{r} = (\boldsymbol{r}_i)_{i=1}^m = ([x_i, y_i])_{i=1}^m$, let d^2 be the sum of the squared residual errors between the data points and their corresponding points on the B-spline curve, i.e.,

$$d^2 = \sum_{i=1}^m \|\mathbf{r}_i - \mathbf{p}(t_i)\|^2 = \sum_{i=1}^m \left[\mathbf{r}_i - \sum_{j=0}^{n+3} \mathbf{B}_{j,4}(t_i) \cdot \mathbf{\Phi}_j \right]^2. \qquad (4)$$

From the cyclical condition of control points in (3), there are only $n + 1$ control points to be estimated. The least square (LS) estimation of the $n + 1$ control points are obtained from the curve points by minimizing d^2 in (4) with respect to $\mathbf{\Phi} = [\mathbf{\Phi}_x^T, \mathbf{\Phi}_y^T]^T = [\Phi_{x0}, \ldots, \Phi_{xn}, \Phi_{y0}, \ldots, \Phi_{yn}]^T$. By factorization of B-spline, two separate solutions are obtained in matrix as follows:

$$\begin{cases} \mathbf{\Phi}_x = [\boldsymbol{B}^T \boldsymbol{B}]^{-1} \boldsymbol{B}^T \boldsymbol{x} \\ \mathbf{\Phi}_y = [\boldsymbol{B}^T \boldsymbol{B}]^{-1} \boldsymbol{B}^T y \end{cases} \qquad (5)$$

where $\mathbf{x} = [x_1, \ldots, x_m]^T, \boldsymbol{y} = [y_1, \ldots, y_m]^T$, $\mathbf{B}$ is shown in the equation at the bottom of the next page, and $\bar{B}_{j,4}^i = B_{j,4}(t_i)$.

Here, we adopt the chord length method, which is the most popular one, for the parameterization of the B-spline. The chord length L of a curve is calculated as follows:

$$L = \sum_{i=2}^{m+1} \|\mathbf{r}_i - \mathbf{r}_{i-1}\| \qquad (6)$$

where $\mathbf{r}_{m+1} = \mathbf{r}_1$ for a closed curve. The t_i associated with the point q_i is given as

$$t_i = t_{i-1} + \frac{\|\mathbf{r}_i - \mathbf{r}_{i-1}\|}{L} \cdot t_{\max} \tag{7}$$

where $t_1 = 0$ and $t_{\max} = n + 1$.

C. Model Selection With Improved BIC Criterion

It is known that for a given set of measurement data, there exists a model of optimal complexity corresponding to the smallest prediction (generalization) error for further data. The complexity of a B-spline model of a surface is related to its control point (parameter) number [13]. If the B-spline model is too complicated, the approximated B-spline surface tends to over-fit noisy measurement data. If the model is too simple, then it is not capable of fitting the measurement data, making the approximation results under-fitted. The problem of finding an appropriate model, referred to as model selection, is important for achieving a high level generalization capability. Model selection has been studied from various standpoints in the field of statistics, including information statistics, Bayesian statistics, and structural risk minimization. The Bayesian approach [14], [15] is perhaps the most general and most powerful model-selection method. Based on posterior model probabilities, the Bayesian approach estimates a probability distribution over an ensemble of models. The prediction is accomplished by averaging over the ensemble of models. Accordingly, the uncertainty of the models is taken into account, and complex models with more degrees of freedom (DOFs) are penalized.

Given a set of models $\{M_k, k = 1, 2, \ldots, k_{\max}\}$ and data $\mathbf{r}$, the Bayesian approach selects the model with the largest posterior probability. The posterior probability of model M_k is

$$p(M_k \mid \mathbf{r}) = \frac{p(\mathbf{r} \mid M_k)p(M_k)}{\sum_{L=1}^{k_{\max}} p(\mathbf{r} \mid M_L)p(M_L)} \tag{8}$$

where $p(\mathbf{r} \mid M_k)$ is the integrated likelihood of model M_k and $p(M_k)$ is the prior probability of model M_k. To find the model with the largest posterior probability, we evaluate $p(M_k \mid \mathbf{r})$ for $k = 1, 2, \ldots, k_{\max}$ and select the model that has the maximum $p(M_k \mid \mathbf{r})$, that is

$$\begin{aligned} M &= \arg \max_{M_k, k=1,\ldots,k_{\max}} \{p(M_k \mid \mathbf{r})\} \\ &= \arg \max_{M_k, k=1,\ldots,k_{\max}} \left\{ \frac{p(\mathbf{r} \mid M_k)p(M_k)}{\sum_{L=1}^{k_{\max}} p(\mathbf{r} \mid M_L)p(M_L)} \right\}. \end{aligned} \tag{9}$$

Here, we assume that the models have the same likelihood *a priori*, so that $p(M_k) = 1/k_{\max}, (k = 1, \ldots, k_{\max})$. Therefore, the model selection in (8) will not be affected by $p(M_k)$. This is also the case with $\sum_{L=1}^{k_{\max}} p(r \mid M_L)p(M_L)$, since it is not a function of M_k. Consequently, we can ignore the factors $p(M_k)$

and $\sum_{L=1}^{k_{\max}} p(r \mid M_L)p(M_L)$ in computing the model criteria. Equation (9) then becomes

$$M = \arg \max_{M_k, k=1,\ldots,k_{\max}} \{p(\mathbf{r} \mid M_k)\}. \tag{10}$$

To calculate the posterior probability of model M_k, we need to evaluate the marginal density of data for each model $p(\mathbf{r} \mid M_k)$, which requires multidimensional integration

$$p(\mathbf{r} \mid M_k) = \int_{\mathbf{\Phi}_k} p(\mathbf{r} \mid \mathbf{\Phi}_k, M_k)p(\mathbf{\Phi}_k \mid M_k)d\mathbf{\Phi}_k \tag{11}$$

where $\mathbf{\Phi}_k$ is the parameter vector for model M_k, $p(\mathbf{r} \mid \mathbf{\Phi}_k, M_k)$ is the likelihood and $p(\mathbf{\Phi}_k \mid M_k)$ is the prior distribution for model M_k.

In practice, calculating the multidimensional integration is very hard, especially for obtaining a closed-form analytical solution. The research in this area has resulted in many approximation methods for achieving this. The Laplace approximation method for the integration appears to be a simple one and has become a standard method for calculating the integration of multivariable Gaussians [14]. This gives

$$\begin{aligned} p(\mathbf{r} \mid M_k) &= \int_{\mathbf{\Phi}_k} p(\mathbf{r} \mid \mathbf{\Phi}_k, M_k)p(\mathbf{\Phi}_k \mid M_k)d\mathbf{\Phi}_k \\ &\cong (2\pi)^{d_k/2}|H(\hat{\mathbf{\Phi}}_k)|^{-1/2}p(\mathbf{r} \mid \hat{\mathbf{\Phi}}_k, M_k)p(\hat{\mathbf{\Phi}}_k \mid M_k) \end{aligned} \tag{12}$$

where $\hat{\mathbf{\Phi}}_k$ is the maximum likelihood estimate of $\mathbf{\Phi}_k$, d_k denotes the number of parameters (control points for B-spline model) in model M_K, and $H(\hat{\mathbf{\Phi}}_k)$ is the Hessian matrix of $-\log p(\mathbf{r}|\mathbf{\Phi}_k, M_k)$ evaluated at $\hat{\mathbf{\Phi}}_k$

$$H(\hat{\mathbf{\Phi}}_k) = - \left. \frac{\partial^2 \log p(\mathbf{r} \mid \mathbf{\Phi}_k, M_k)}{\partial \mathbf{\Phi}_k \partial \mathbf{\Phi}_k^T} \right|_{\mathbf{\Phi}_k=\hat{\mathbf{\Phi}}_k}. \tag{13}$$

This approximation is particularly good when the likelihood function is highly peaked around $\hat{\mathbf{\Phi}}_k$. This is usually the case when the number of data samples is large. Neglecting the terms of $p(\hat{\mathbf{\Phi}}_k|M_k)$ and using log in the calculation, the posterior probability of model M_k becomes

$$M = \arg \max_{M_k, k=1,\ldots,k_{\max}} \left\{ \log p(\mathbf{r} \mid \hat{\mathbf{\Phi}}_k, M_k) - \frac{1}{2}\log|H(\hat{\mathbf{\Phi}}_k)| \right\}. \tag{14}$$

The likelihood function $p(\mathbf{r}|\hat{\mathbf{\Phi}}_k, M_k)$ of a closed B-spline cross section curve can be factored into x and y components as

$$p(\mathbf{r} \mid \hat{\mathbf{\Phi}}_k, M_k) = p(\mathbf{x} \mid \hat{\mathbf{\Phi}}_{kx}, M_k) \cdot p(\mathbf{y} \mid \hat{\mathbf{\Phi}}_{ky}, M_k) \tag{15}$$

where $\hat{\mathbf{\Phi}}_{kx}$ and $\hat{\mathbf{\Phi}}_{ky}$ can be calculated by (5).

$$\mathbf{B} = \begin{bmatrix} \bar{B}_{0,4}^1 + \bar{B}_{n+1,4}^1 & \bar{B}_{1,4}^1 + \bar{B}_{n+2,4}^1 & \bar{B}_{2,4}^1 + \bar{B}_{n+3,4}^1 & \cdots & \bar{B}_{n,4}^1 \\ \bar{B}_{0,4}^2 + \bar{B}_{n+1,4}^2 & \bar{B}_{1,4}^2 + \bar{B}_{n+2,4}^2 & \bar{B}_{2,4}^2 + \bar{B}_{n+3,4}^2 & \cdots & \bar{B}_{n,4}^2 \\ \vdots & \vdots & \vdots & \vdots & \vdots \\ \bar{B}_{0,4}^m + \bar{B}_{n+1,4}^m & \bar{B}_{1,4}^m + \bar{B}_{n+2,4}^m & \bar{B}_{2,4}^m + \bar{B}_{n+3,4}^m & \cdots & \bar{B}_{n,4}^m \end{bmatrix}$$

Consider the x component. Assuming that the residual error sequence is zero mean and white Gaussian with variance $\sigma_{kx}^2(\hat{\boldsymbol{\Phi}}_{kx})$, we have the following likelihood function:

$$p(\mathbf{x} \,|\, \hat{\boldsymbol{\Phi}}_{kx}, M_k) = \left(\frac{1}{2\pi\sigma_{kx}^2(\hat{\boldsymbol{\Phi}}_{kx})}\right)^{m/2} \exp\left\{-\frac{1}{2\sigma_{kx}^2(\hat{\boldsymbol{\Phi}}_{kx})} \sum_{k=0}^{m-1} [x_k - \mathbf{B}_k\hat{\boldsymbol{\Phi}}_{kx}]^2\right\}$$

(16)

with $\sigma_{kx}^2(\hat{\boldsymbol{\Phi}}_{kx}, M_k)$ estimated by

$$\hat{\sigma}_{kx}^2(\hat{\boldsymbol{\Phi}}_{kx}) = \frac{1}{m} \sum_{k=0}^{m-1} [x_k - \mathbf{B}_k\hat{\boldsymbol{\Phi}}_{kx}]^2. \qquad (17)$$

Similarly, the likelihood function of the y component can also be obtained. The corresponding Hessian matrix $\hat{H}_k$ of $-\log p(\mathbf{r}|\boldsymbol{\Phi}_k, M_k)$ evaluated at $\hat{\boldsymbol{\Phi}}_k$ is

$$H(\hat{\boldsymbol{\Phi}}_k) = \begin{bmatrix} \frac{\mathbf{B}^T\mathbf{B}}{\hat{\sigma}_{kx}^2(\hat{\boldsymbol{\Phi}}_{kx})} & \mathbf{0} \\ \mathbf{0} & \frac{\mathbf{B}^T\mathbf{B}}{\hat{\sigma}_{ky}^2(\hat{\boldsymbol{\Phi}}_{ky})} \end{bmatrix}. \qquad (18)$$

Approximating $(1/2)\log|H(\hat{\boldsymbol{\Phi}}_k)|$ by the asymptotic expected value of Hessian $(1/2)(d_{kx} + d_{ky})\log(m)$, we can obtain the BIC for selecting the structure of B-spline curve

$$M = \arg \max_{M_k, k=1,\ldots,k_{\max}} \left\{\begin{array}{c} -\frac{m}{2}\log\hat{\sigma}_{kx}^2(\hat{\boldsymbol{\Phi}}_{kx}) - \frac{m}{2}\log\hat{\sigma}_{ky}^2(\hat{\boldsymbol{\Phi}}_{ky}) \\ -\frac{1}{2}(d_{kx}+d_{ky})\log(m) \end{array}\right\}$$

(19)

where d_{kx} and d_{ky} are the number of control points in x and y directions, respectively, m is the number of data points.

In the conventional BIC criterion as shown in (19), the first two terms measure the estimation accuracy of the B-spline model. In general, the variance $\hat{\sigma}_k^2$ estimated from (17) tends to decrease with the increase in the number of control points. The smaller the variance value in $\hat{\sigma}_k^2$, the bigger the value of the first two terms (as the variance is much smaller than one) and, therefore, the higher the order (i.e., the more the control points) of the model resulting from (19). However, if too many control points are used, the B-spline model will over-fit noisy data points. An over-fitted B-spline model will have poor generalization capability. Model selection, thus, should achieve a proper tradeoff between the approximation accuracy and the number of control points of the B-spline model. With a conventional BIC criterion, the same data set is used for estimating both the control points of the B-spline model and the variances. Thus, the first two terms in (19) cannot detect the occurrence of over-fitting in the B-spline model selected. In theory, the third term in (19) could penalize over-fitting as it appears directly proportional to the number of control points used. In practice, however, we note from our experiences that the effect of this penalty term is insignificant, compared with that of the first two terms. As a result, the conventional BIC criterion is rather insensitive to the occurrence of over-fitting and tends to select more control points in the B-spline model to approximate the data point, which normally results in a model with poor generalization capability.

The reason for the occurrence of over-fitting in the conventional BIC criterion lies in the way the variances σ_{kx}^2 and σ_{ky}^2

are obtained. A reliable estimate of σ_{kx}^2 and σ_{ky}^2 should be based on resampling of the data. In other words, the generalization capability of a B-spline model should be validated using another set of data points, rather than the same data used in obtaining the model. To achieve this, we divide the available data into two sets: a training sample and a prediction sample. The training sample is used only for model estimation, whereas the prediction sample is used only for estimating data noise σ_{kx}^2 and σ_{ky}^2. For a candidate B-spline model M_k with d_{kx} and d_{ky} control points in the x and y directions, the BIC in (19) is, thus, evaluated via the following steps:

1) estimate the model parameter $\hat{\boldsymbol{\Phi}}_k$ using the training sample by (5).
2) estimate the data noise σ_k^2 using the prediction sample by (17).

If the model $\hat{\boldsymbol{\Phi}}_k$ fitted to the training data is valid, then the estimated variance $\hat{\sigma}_k^2$ from the prediction sample should also be a valid estimate of the data noise. If the variance $\hat{\sigma}_k^2$ found from the prediction sample is unexpectedly large, we have reasons to believe that the candidate model fits the data badly. It is seen that the data noise $\hat{\sigma}_k^2$ estimated from the prediction sample will, thus, be more sensitive to the quality of the model than the one directly estimated from training sample, as the variance σ_k^2 estimated from the prediction sample also has the capability of detecting the occurrence of over-fitting.

III. UNCERTAINTY ANALYSES

In Section II, we described our approach to model selection and parameter estimation in the framework of Bayesian statistics. In this section, we will discuss how the same framework for B-spline curve approximation relates to the task of selecting the NBV for acquiring new data. For simplification of description, we will replace $\boldsymbol{\Phi}_k$ by $\boldsymbol{\Phi}$ to show that we are dealing with the selected "best" B-spline model with d_{kx} and d_{ky} control points. To obtain the approximate B-spline model, we will predict the distribution of the information gain about the model's parameter $\boldsymbol{\Phi}$ along each cross section curve. A measure of the information gain will be designed, whose expected value will be maximal when the new measurement data are acquired. The measurement is based on Shannon's entropy whose properties make it a sensible information measure here. We will describe the information entropy of the B-spline model and how to use it to achieve maximal information gain about the parameters $\boldsymbol{\Phi}$ of the B-spline model.

A. Information Entropy of a B-Spline Model

Given $\boldsymbol{\Phi}$ and the data points $\mathbf{r} = (\mathbf{r}_i)_{i=1}^m$ assumed to be statistically independent, with Gaussian noise of zero mean and variance σ^2, the joint probability of $\mathbf{r} = (\mathbf{r}_i)_{i=1}^m$ is

$$p(\mathbf{r} \,|\, \boldsymbol{\Phi}) = \frac{1}{(2\pi\sigma^2)^{m/2}} \cdot \exp\left[-\frac{1}{2\sigma^2}(\mathbf{r} - \mathbf{B}\cdot\boldsymbol{\Phi})^T(\mathbf{r} - \mathbf{B}\cdot\boldsymbol{\Phi})\right]. \quad (20)$$

Equation (20) has an asymptotic approximation representation defined by [16]

$$p(\mathbf{r} \,|\, \boldsymbol{\Phi}) \approx p(\mathbf{r} \,|\, \hat{\boldsymbol{\Phi}})\exp\left[-\frac{1}{2}(\boldsymbol{\Phi} - \hat{\boldsymbol{\Phi}})^T H_m(\boldsymbol{\Phi} - \hat{\boldsymbol{\Phi}})\right] \quad (21)$$

where $\hat{\boldsymbol{\Phi}}$ is the maximum-likelihood estimation of $\boldsymbol{\Phi}$ given the data points, and H_m is the Hessian matrix of $-\log p(\mathbf{r}|\boldsymbol{\Phi})$ evaluated at $\hat{\boldsymbol{\Phi}}$ given data points $\mathbf{r} = (\mathbf{r}_i)_{i=1}^m$.

The *a posteriori* distribution $p(\boldsymbol{\Phi}\,|\,\mathbf{r})$ of the given data is approximately proportional to

$$p(\boldsymbol{\Phi}\,|\,\mathbf{r}) \approx p(\mathbf{r}\,|\,\hat{\boldsymbol{\Phi}})$$
$$\cdot \exp\left[-\frac{1}{2}(\boldsymbol{\Phi} - \hat{\boldsymbol{\Phi}})^T H_m (\boldsymbol{\Phi} - \hat{\boldsymbol{\Phi}})\right] p(\boldsymbol{\Phi}) \quad (22)$$

where the $p(\boldsymbol{\Phi})$ is the *a priori* probability of the B-spline model parameters. If the *a priori* has a Gaussian distribution with mean $\hat{\boldsymbol{\Phi}}$ and covariance H_m^{-1}, we have

$$p(\boldsymbol{\Phi}\,|\,\mathbf{r}) \propto \exp\left[-\frac{1}{2}(\boldsymbol{\Phi} - \hat{\boldsymbol{\Phi}})^T H_m (\boldsymbol{\Phi} - \hat{\boldsymbol{\Phi}})\right]. \quad (23)$$

From Shannon's information entropy, the conditional entropy of $p(\boldsymbol{\Phi}\,|\,\mathbf{r})$ is defined by

$$E_m(\boldsymbol{\Phi}) = \int p(\boldsymbol{\Phi}\,|\,\mathbf{r}) \cdot \log p(\boldsymbol{\Phi}\,|\,\mathbf{r})\, d\boldsymbol{\Phi}. \quad (24)$$

If $p(\boldsymbol{\Phi}\,|\,\mathbf{r})$ obeys Gaussian distribution, the corresponding entropy is [17]

$$E_m = \Delta + \frac{1}{2}\log\left(\det H_m^{-1}\right) \quad (25)$$

where Δ is a constant.

The entropy in (25) measures the information about the B-spline model parameters, given data points $(\mathbf{r}_1, \ldots, \mathbf{r}_m)$. The more information about $\boldsymbol{\Phi}$, the smaller the entropy will be. In this paper, we use the entropy in (25) as the measurement of the uncertainty of the model parameter $\boldsymbol{\Phi}$. Thus, to minimize E_m, we will make $\det H_m^{-1}$ as small as possible.

B. Information Gain

In order to predict the distribution of the information gain, we assume a new data point $\mathbf{r}_{m+1}$ collected along a contour. The potential information gain is determined by incorporating the new data point $\mathbf{r}_{m+1}$. If we move the new point $\mathbf{r}_{m+1}$ along the contour, the distribution of the potential information gain along the whole contour can be obtained. Now, we will derive the relationship between the information gain and the new data point $\mathbf{r}_{m+1}$.

Assume that a new data point $\mathbf{r}_{m+1}$ has been collected. Let $P(\boldsymbol{\Phi}|\mathbf{r}_1, \ldots, \mathbf{r}_m, \mathbf{r}_{m+1})$ be the probability distribution of model parameter $\boldsymbol{\Phi}$ after a new point $\mathbf{r}_{m+1}$ is added. Its corresponding entropy is $E_{m+1} = \Delta + \frac{1}{2}\log\left(\det \hat{H}_{m+1}^{-1}\right)$. The information gain then is

$$\Delta E = E_m - E_{m+1} = \frac{1}{2}\log\frac{\det H_m^{-1}}{\det H_{m+1}^{-1}}. \quad (26)$$

From (18), the new data point $\mathbf{r}_{m+1}$ will incrementally update the Hessian matrix as follows:

$$H_{m+1} \approx H_m + \begin{bmatrix} \frac{1}{\sigma_x^2} \cdot \bar{B}_{m+1}^T \bar{B}_{m+1} & \mathbf{0} \\ \mathbf{0} & \frac{1}{\sigma_y^2} \cdot \bar{B}_{m+1}^T \bar{B}_{m+1} \end{bmatrix} \quad (27)$$
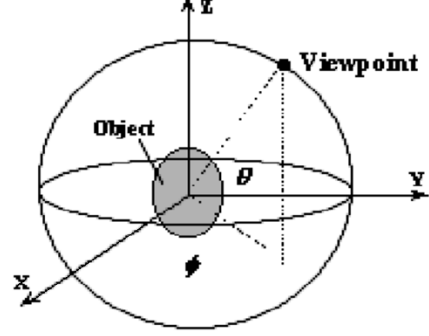

Fig. 2. Viewpoint representation.

where $\hat{\sigma}_{m+1}^2 \approx \hat{\sigma}_m^2$. $\bar{B}_{m+1}$ is defined by

$$\bar{B}_{m+1} = \left[\bar{B}_{0,4}^{m+1} + \bar{B}_{n+1,4}^{m+1}, \bar{B}_{1,4}^{m+1} + \bar{B}_{n+2,4}^{m+1}, \ldots, \bar{B}_{n,4}^{m+1}\right].$$

The determinant of H_{m+1}

$$\det H_{m+1}$$
$$\approx \det\left[\mathbf{I} + \begin{bmatrix} \frac{1}{\hat{\sigma}_x^2} \cdot \bar{B}_{m+1}^T \bar{B}_{m+1} & \mathbf{0} \\ \mathbf{0} & \frac{1}{\hat{\sigma}_y^2} \cdot \bar{B}_{m+1}^T \bar{B}_{m+1} \end{bmatrix} H_m^{-1}\right]$$
$$\cdot \det H_m$$

can be simplified to

$$\det H_{m+1} \approx \left(1 + \bar{B}_{m+1} \cdot [\mathbf{B}^T \mathbf{B}]^{-1} \cdot \bar{B}_{m+1}^T\right)^2 \cdot \det H_m. \quad (28)$$

Since $\det H^{-1} = 1/\det H$, (26) can be simplified to

$$\Delta E = \log\left(1 + \bar{B}_{m+1} \cdot [\mathbf{B}^T \mathbf{B}]^{-1} \cdot \bar{B}_{m+1}^T\right). \quad (29)$$

Assuming that the new additional data point $\mathbf{r}_{m+1}$ travels along the contour, the resulting potential information gain of the B-spline model will change, according to (29). In order to reduce the uncertainty of the model, we would like to have the new data point at such location that the potential information gain attainable is largest. Therefore, after reconstructing the section curve by fitting partial data acquired from previous viewpoints, the NBV should be selected as the one that sense those new data points which give the largest possible potential information gain for the B-spline model.

IV. NEXT BEST VIEW

A. View Space Representation

A view space is a set of 3-D positions where the sensor (vision system) takes measurements. We assume that the 3-D object is within the field of view and the depth of view of the vision system. The optical settings of the vision system are fixed. Based on these assumptions, the parameters of the vision system to be planned are the viewing pose of the sensor. In this section, the candidate viewpoints are represented in a spherical viewing space. The view space is usually a continuous spherical surface. To reduce the number of viewpoints used in practice, we discretize the surface by using the icosahedron method. In addition, we assume that the view space is centered around the object, and its radius is equal to *a priori* specified distance from the sensor to the object. As shown in Fig. 2, since the optical axis of the sensor passes through the center of

the object, the viewpoint can be represented by pan-tilt angles $\phi([-180°, 180°])$ and $\theta([-90°, 90°])$.

According to the representation of the viewing space, the fundamental task in the view planning here is to obtain the visibility regions in the viewing space that contain the candidate viewpoints where the missing information about the 3-D object can be obtained without occlusions. The NBV should be the viewpoint that can give maximum information about the object.

B. Viewpoint Evaluation

With the above view space representation, we can now map the predicted information gain to the view space for viewpoint planning. For a viewpoint $v(\theta, \phi)$, we say one data point on the object is visible if the angle between its normal and the view direction is smaller than a breakdown angle α of the sensor. The view space V_k for each data point $\mathbf{r}_k, (k = 1, 2, \ldots)$ is the set of all possible viewpoints that can see $\mathbf{r}_k$. The view space V_k can be calculated via the following procedure.

1) Calculating the normal vector $\mathbf{n}_k$ of a point $\mathbf{r}_k(k = 1, 2, \ldots)$ on the object, using a LS error fitting of a 3×3 local surface patch in its neighborhood.
2) Extracting viewpoints from which $\mathbf{r}_k$ is visible. These viewpoints are denoted as view space V_k.

After the view space $V_k, (k = 1, 2, \ldots)$ is extracted, we construct a measurement matrix $\mathbf{M}$. The components $m_{k,j}$ of an l-by-w measurement matrix is given as

$$m_{k,j} = \begin{cases} \langle \mathbf{n}_k \cdot \mathbf{v}_j \rangle, & \text{if } \mathbf{r}_k \text{ is visible to } v_j \\ 0, & \text{otherwise} \end{cases} \quad (30)$$

where $\mathbf{v}_j$ is the direction vector of viewpoint v_j.

Then, for each view $v(\theta, \phi)$, we define a global measure of the information gain $I(\theta, \phi)$ as the criterion to be summed over all visible surface points seen under this view of the sensor. $I(\theta, \phi)$ is defined by

$$I_j(\theta_j, \phi_j) = \sum_{k \in R_j} m_{k,j} \cdot \Delta E_k \quad (31)$$

where ΔE_k is the information gain at surface point $\mathbf{r}_k$, which is weighted by $m_{k,j}$.

Therefore, the NBV (θ^*, ϕ^*) is one that maximizes the information gain function of $I(\theta, \phi)$

$$(\theta^*, \phi^*) = \max_{\theta_j, \phi_j} I_j(\theta_j, \phi_j). \quad (32)$$

V. EXPERIMENTS

The information entropy based viewpoint-planning algorithm is implemented as part of the work for 3-D object reconstruction. The setup of a general 3-D shape measurement system is schematically shown in Fig. 3. The sensor mounted on a robot consists of a projector that projects structured light onto the object and a charge-coupled device (CCD) camera that captures the image of the illuminated object surface [2]. This range sensor can give depth information of the scanned surface of an object in the form of "data cloud." In the current implementation, the object is placed on a stationary platform. The robot has 6 DOFs and is able to take a measurement of the object from any viewing pose specified within its work space. The modeling
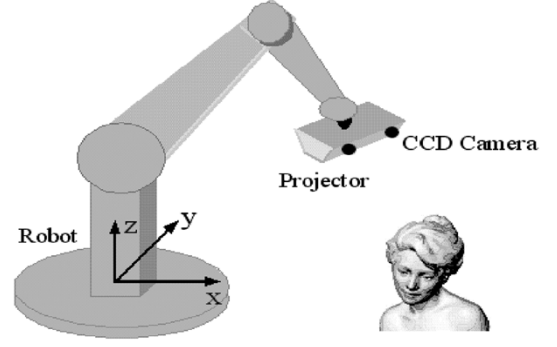

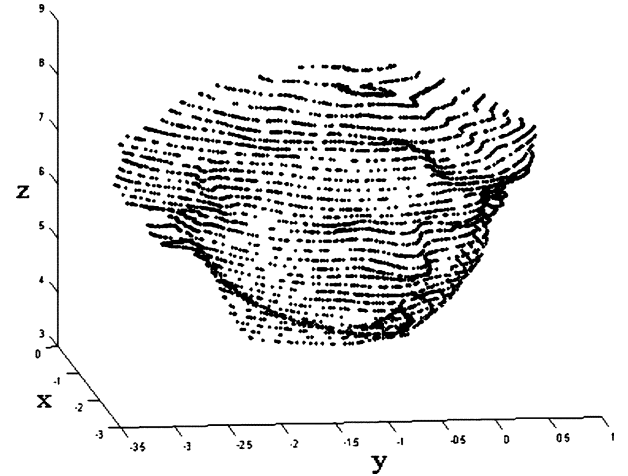
Fig. 3.   System setup.

Fig. 4.   Cross section curves after preprocessing.

process for a 3-D object consists of a sequence of four repeated steps: acquiring data of the object surface from a viewpoint, registering the acquired data, integrating the new data with the partial model, and determining the NBV. This cycle will be repeated until the NBV terminates.
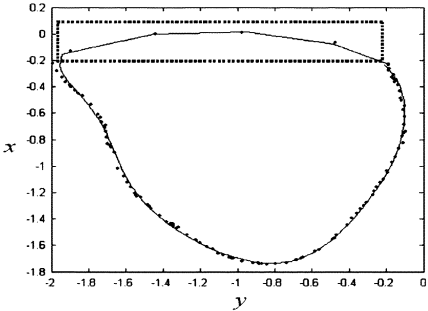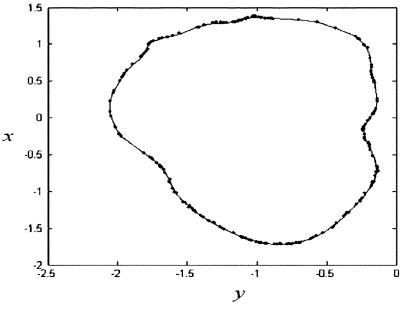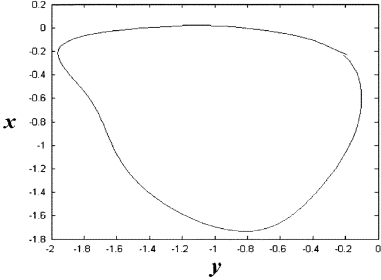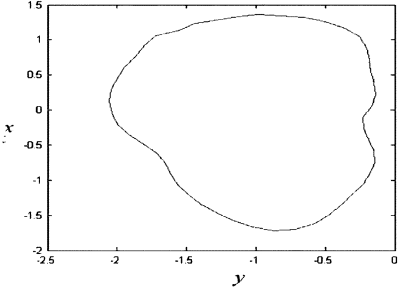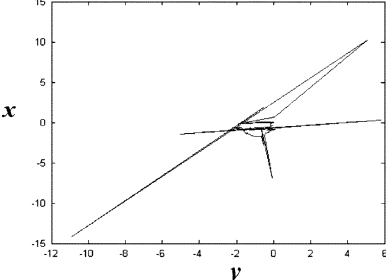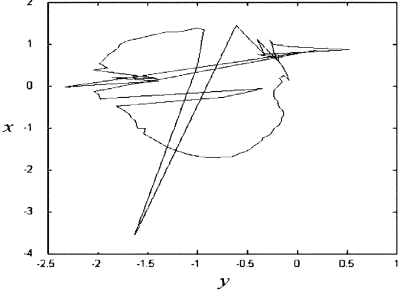
To slice the acquired "data cloud," we define an interval distance between cross section curves in a certain direction (e.g., z direction) and project the data in the neighborhood of each cross section curve onto the plane on which the cross section curve lies. The preprocessing results of the 3-D "data cloud" are shown in Fig. 4. Here, the interval between two cross section curves was set as 1.5 mm and the neighborhood of each cross section curve is set as 0.2 mm.

These points projected onto a cross section curve were distributed randomly. They need to be sorted out before the curve reconstruction can be performed. For each section curve, these projected points were transformed into polar coordinate system. The phase angle was used to sort these points. To reconstruct these cross section curves via B-splines, we need to select an appropriate model structure first. The model selection is important for automated 3-D modeling, to account for the data already acquired and to avoid over-fitting of the model.

A. Model Selection

In this section, the improved BIC criterion proposed will be used to select the B-spline model to represent the cross section

TABLE I
COMPARISON OF THE RESULTS OF OUR IMPROVED BIC WITH CONVENTIONAL BIC.
IN THE CASES OF PARTIAL DATA AND COMPLETE DATA AVAILABLE, RESPECTIVELY

	In the case of partial data available	In the case of complete data available
Cross section data		
Verification results by our improved BIC	Model complexity: 9 Estimation accuracy: 0.0406 	Model complexity: 53 Estimation accuracy: 0.0049
Verification results by conventional BIC	Model complexity: 150 Estimation accuracy: 1.8015 	Model complexity: 147 Estimation accuracy: 0.3811

curves. Two cross section curves from a series of sliced cross section curves will be used as examples to demonstrate the effectiveness of our approach. To evaluate the selected models, the following performance indexes are used.

1) *Model complexity*, which refers to the number of control points of the B-spline model.
2) *Estimation accuracy*, which is defined as the mean squared errors (MSEs) between the actual data points and the reconstructed model chosen by a selection criterion.

The model complexity and estimation accuracy provide insights into the appropriateness of model fitting (i.e., over-fitting or under-fitting). In the current implementation, uniform B-spline is used for reconstructing the cross section curves, whose control points are uniformly distributed in the interval between the two end points of the curve in the parameter space. In selecting the model for a cross section curve, the number

of control point is iteratively incremented by one from the initial minimum number, while the corresponding BIC value is evaluated using (19). The minimum number of control points of a B-spline model is normally set as six here.

We first conducted experiments with only partial data of an object surface acquired by our range sensor from the first view. The object is the head of a statue as shown in Fig. 4. For each of the cross section curves, some data points were available for its reconstruction. Here, we describe the modeling process via an example in reconstructing one cross section curve. To implement our improved BIC, the available data were first divided into two parts: a training sample set and a prediction sample set. The training sample set was used to estimate the parameters of a candidate B-spline model by (5), followed by the estimation of the variance σ_{kx}^2 and σ_{ky}^2 by (17) using the prediction sample set. The corresponding BIC value for each of the candidate B-spline models was evaluated by (19). The model with
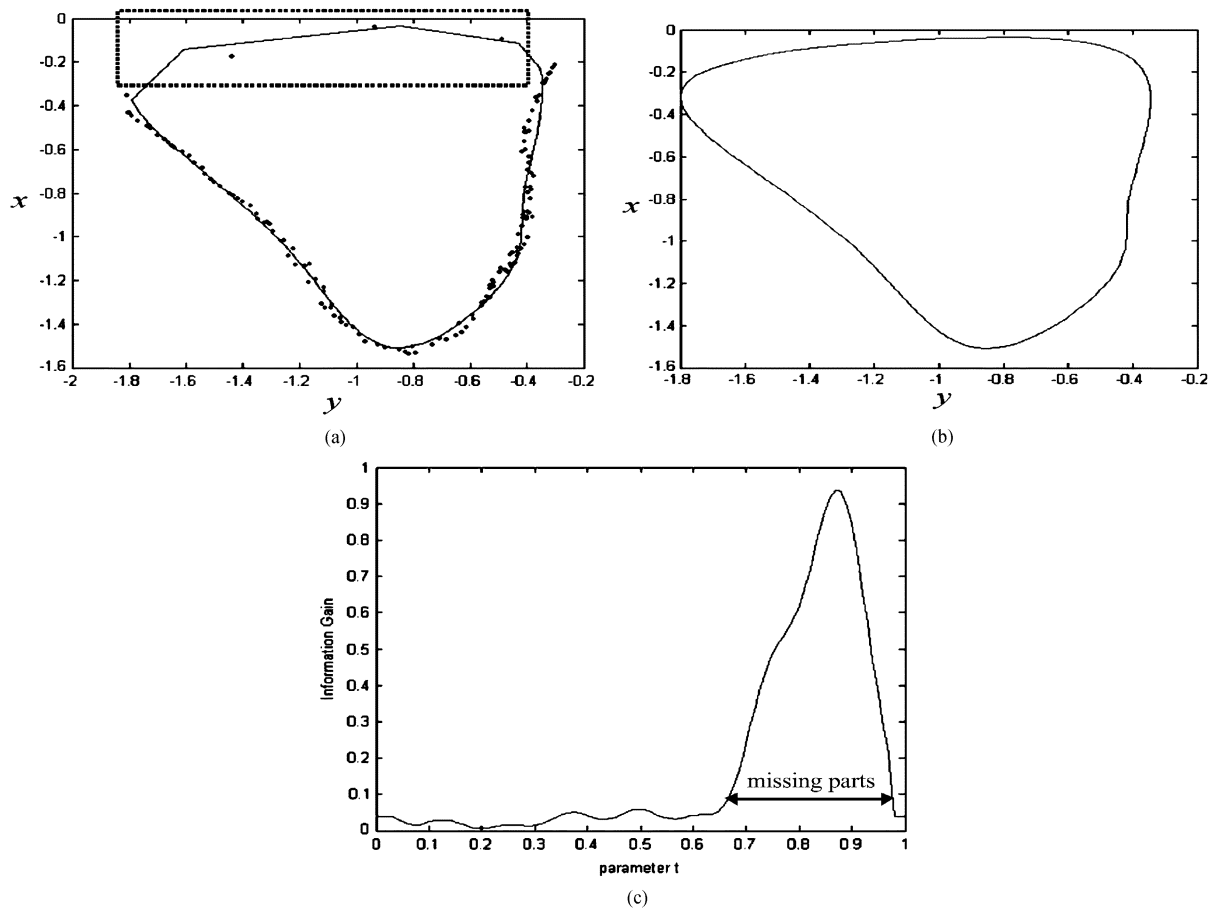
(a)

(b)

(c)

Fig. 5. Reconstruction of cross section curve and predicted potential information gain under the first viewpoint. (a) Data on a cross section curve acquired from the first view. (b) Reconstructed B-spline curve. (c) The potential information gain.
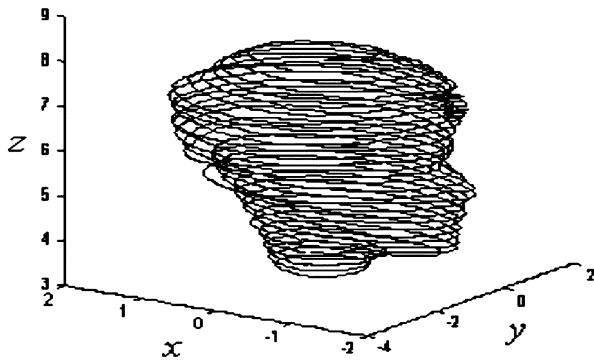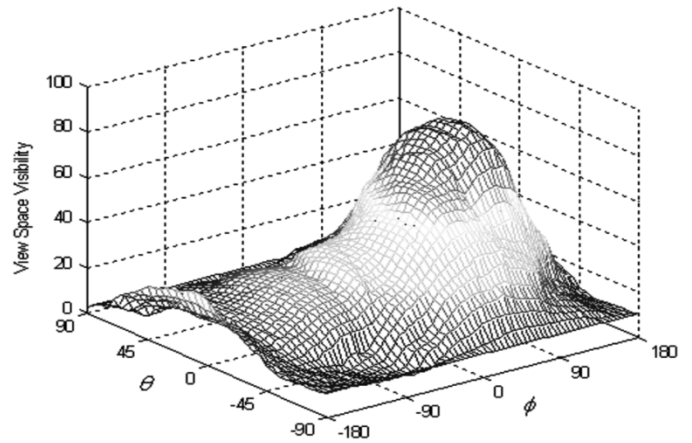

Fig. 6. The reconstructed cross section curves.

Fig. 7. "View space visibility" for the first NBV.

maximum BIC value was selected as the optimal one to approximate the data points, giving the resulting model complexity of nine. This model was then verified by using another set of data on the same cross section. The resulting curve is given in the second row in Table I. The estimation accuracy which is the mean squared errors between the actual data points and the reconstructed model was found to be 0.0406 mm. As a comparison, the conventional BIC was also applied to the same curve. However, all 240 data points were used in selecting the model via evaluating the BIC value by (19), giving the selected model complexity of 150. Again, using another set of data (the same set as used in the above verification), this model was verified, with

the resulting curve given in the third row in Table I. The estimation accuracy in this case was found to be 1.8015 mm. This large error shows that the conventional BIC results in over-fitted approximation for the whole curve via the partial data. This illustrates the limitation of the conventional BIC criterion: its insensitivity to over-fitting. Note that in Table I, the scales of the figures are set differently, which is to show the resulting errors in the reconstructed curves by different criteria which are significantly different in magnitudes. Similar phenomena were observed for other cross section curves. Here, only the results
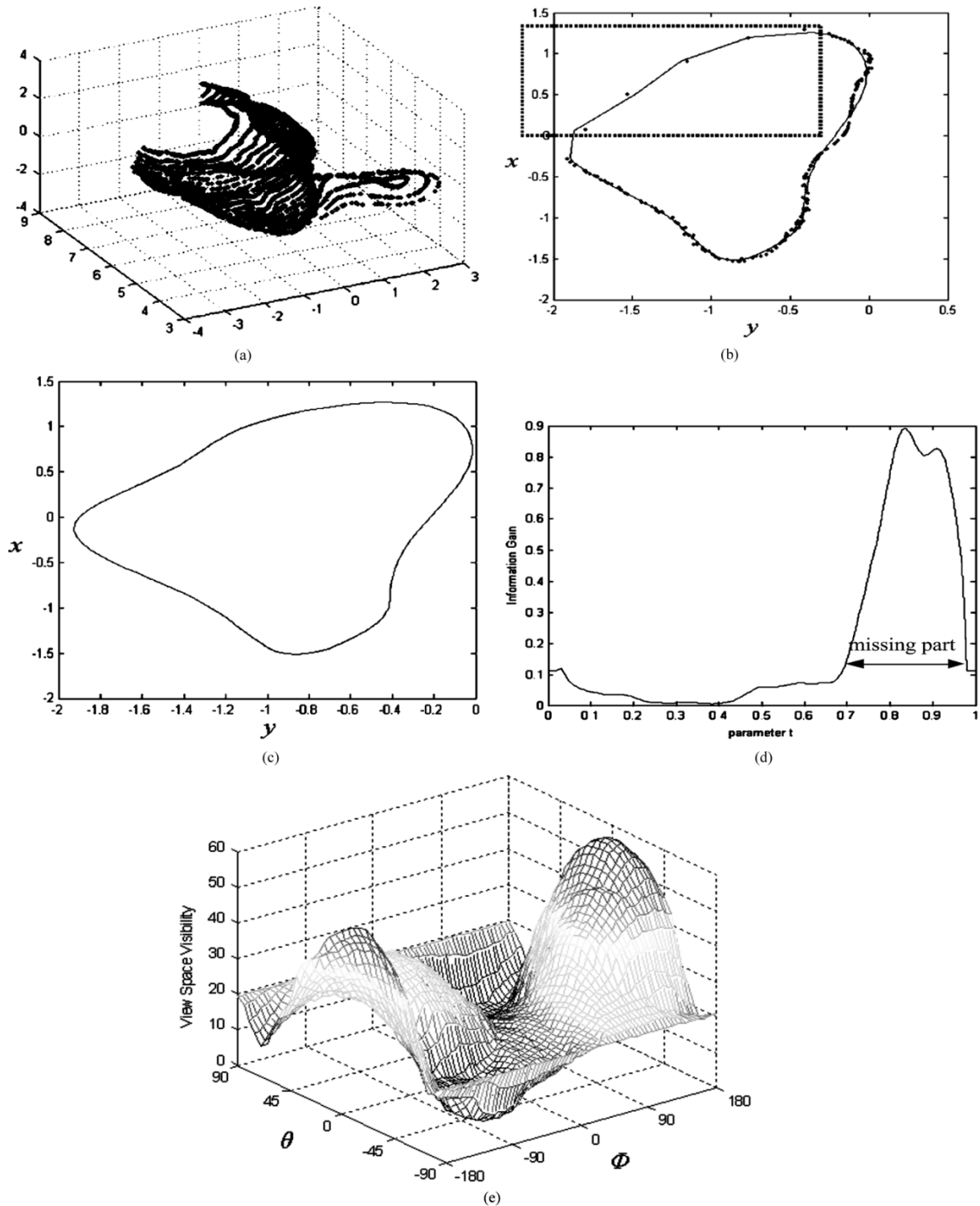
Fig. 8. The process in determining the second NBV. (a) Data acquired from the first two viewpoints after slicing. (b) Data on a cross section acquired from the first two viewpoints. (c) Reconstructed B-spline curve based on the first two viewpoints. (d) The information gain based on the first two viewpoints. (e) "View space visibility" for determining the second NBV.

for one curve are given in Table I. In practical implementation, some physical constraints need to be given. For example, due to self-occlusion, the back of the object will not be visible from the first view. Some points were, thus, defined between the two end points of the available cross section data to limit the range of occluded part of the object. It is useful and reasonable to confine the occluded part of the object within the range of the two end

points of the available data beyond which the part would actually become visible to the current view. These defined points are highlighted in the box in the figures in the first row in Table I.

The second experiment conducted was the one when complete data of a surface were available. The procedures in reconstructing the cross section curves were the same as those in the first experiment. For each section curve, verifications of the
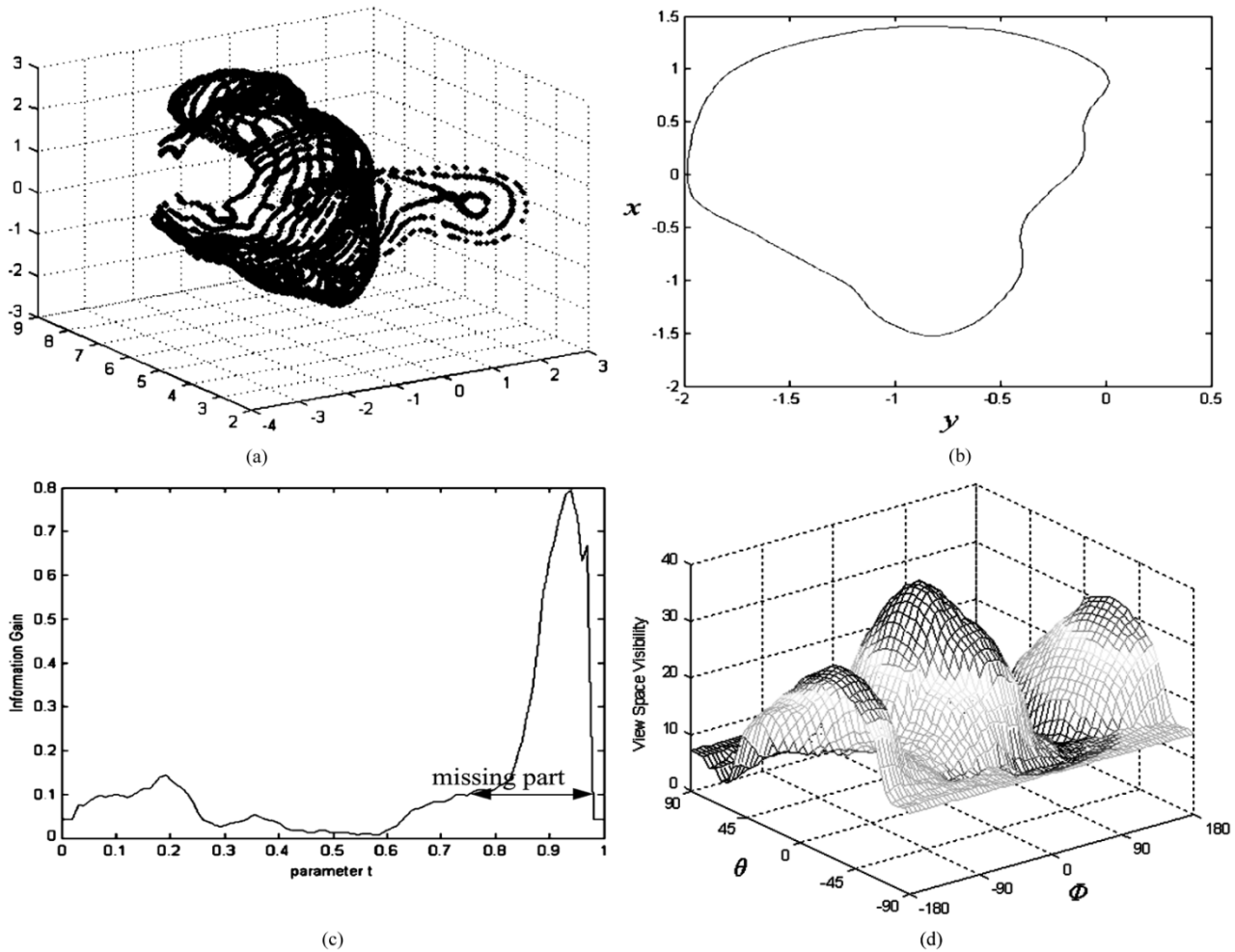
Fig. 9. The process in determining the third NBV. (a) Data acquired from the first three viewpoints. (b) Reconstructed B-spline curve based on the first three viewpoints. (c) The information gain based on the first three viewpoints. (d) "View space visibility" for determining the third NBV.

models reconstructed by the two methods (our improved BIC and conventional BIC) were again conducted using another set of data (different from that used for reconstructing the model) on the same curve, with the results listed in the second column in Table I. From the results, it is observed that even with complete data for a curve, the conventional BIC still results in over-fitted model as seen in the large errors in the verification, while our improved BIC method can reconstruct these cross section curves satisfactorily. With more data available in this experiment, the complexities of the selected models increased using both selection criteria. Yet, the conventional BIC performed poorly with apparent over-fitting in its reconstructed models.

B. Determining the NBV

In Section V-A, we showed how our improved BIC criterion selects the B-spline model for the reconstruction of cross section curves. In this section, we will analyze the uncertainty of the B-spline model selected by our improved BIC for each cross section curve, and predict the information gain of the model along each curve using (29). Based on this analysis, we then map the information gain onto the view space. The view with maximum information gain is selected as the NBV. Then the vision sensor can take another measurement from the NBV to update the B-spline model. We will take one cross section curve as an example to illustrate the process in determining the NBV.

1) Determining the First NBV: First, we take the measurement from an arbitrary initial viewpoint to acquire the first part of data of the unknown object. The data points on one of the cross section curves are shown in Fig. 5(a). The box in Fig. 5(a) contains the points to confine the range of the occluded part of the object. Since these points are few in number, their effects on the predicted information gain of the B-spline model can be ignored. Fig. 5(b) is the reconstructed B-spline model using the partial data acquired from the first viewpoint. This model is a rough approximation for the whole cross section curve. Using this model, we predict the potential information along the reconstructed curve. As shown in Fig. 5(c), the place on the curve where the data are missing (the missing part) corresponds to high potential information gain. This indicates that the occluded part should be given high priority in the next measurement. Note that the information gain [in Fig. 5(c)] is given in the parameter space of the B-spline curve here.

Following the above procedure, each cross section curve is reconstructed in a B-spline model, with the corresponding information gain obtained. Here, each cross section curve is considered to be equally important, so that we can normalize the
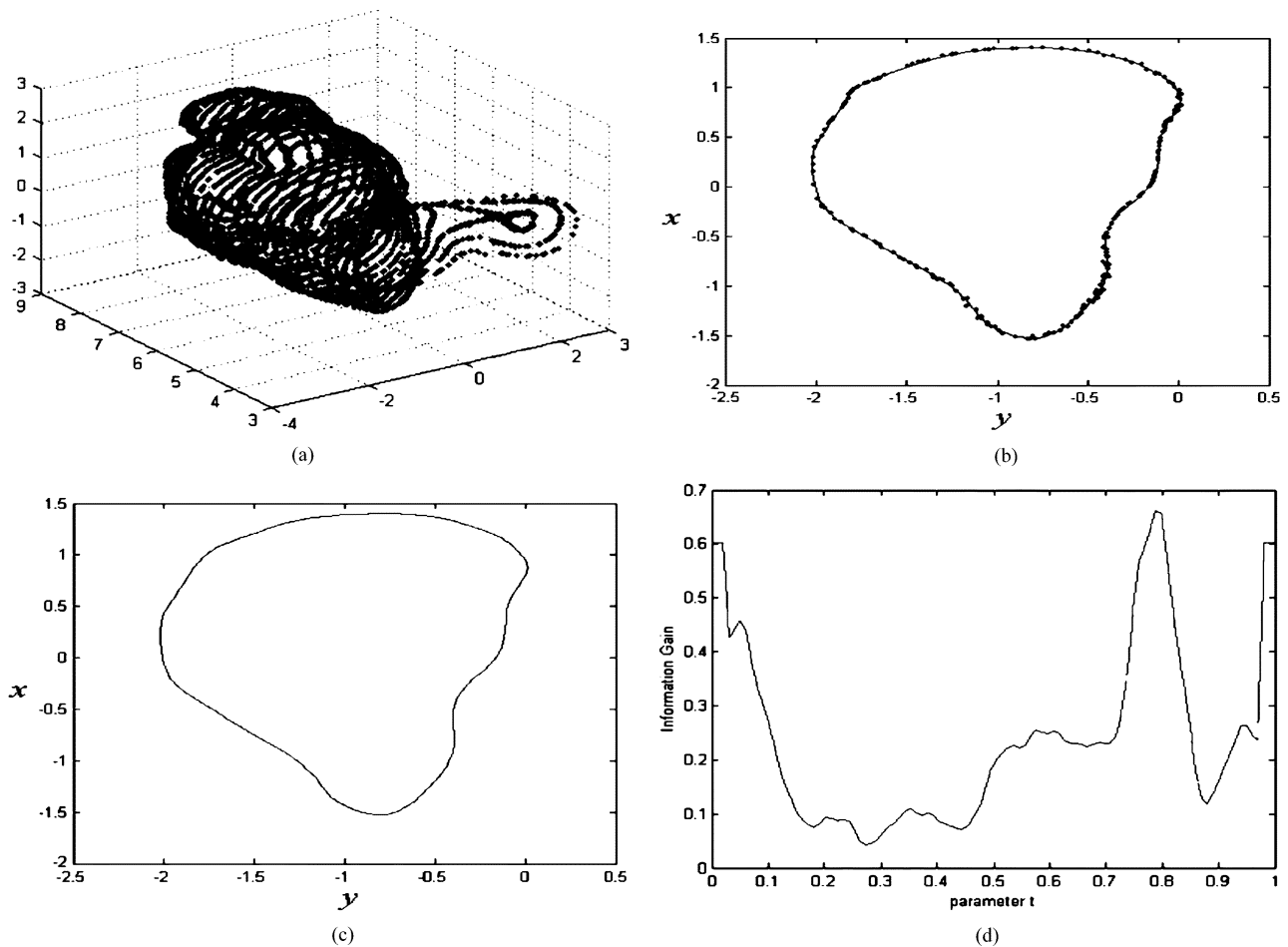
Fig. 10. Reconstruction of a cross section curve and information gain. (a) Data acquired from the first four viewpoints. (b) Data on a cross section curve acquired from the first four viewpoints. (c) Reconstruction result of a cross section curve based on the first four viewpoints. (d) The information gain based on the first four viewpoints.

predicted information gain for each of the cross section curves covered by the current view. Fig. 6 shows all the cross section curves reconstructed from the 3-D data points taken from the first viewpoint.

In the above reconstruction, since only the data points from the first viewpoint are available, the obtained B-spline model cannot describe the whole object accurately. Yet, it enables us to obtain a rough shape and the information gain about the object. Based on the reconstructed partial model, we then map the predicted information gain onto the view space. As a result, we can obtain the relationship between the predicted information gain about the object and the viewpoints, which is also referred to as "View Space visibility." As shown in Fig. 7, the viewpoint at $[-3.0°, 107°]$ that has maximum information gain is, thus, selected as the NBV.

2) Determining Further NBVs: After the first NBV was selected, the robot was commanded to move the vision sensor to this viewpoint to take new measurement. The newly acquired data were then sliced and registered, to give the data acquired from the first two viewpoints as shown in Fig. 8(a).

Using the available data, model selection and information gain prediction were performed following the same procedures as described above. For an example, cross section shown in Fig. 8(b), the newly reconstructed curve is given in Fig. 8(c)

TABLE II
THE RESULTS IN THE VIEW PLANNING FOR THE STATUE

Next Best View	1st viewpoint	1st NBV	2nd NBV	3rd NBV
Model complexity	7	11	22	26
Entropy of B-spline	-15.81	-16.23	-18.95	-19.79

Fig. 11. Final reconstruction result of the statue.

and the updated information gain is given in Fig. 8(d). The predicted information gains for all the cross section curves were then mapped onto the view space, to give the updated view space visibility [shown in Fig. 8(e)] for determining the second NBV. From this view space visibility map, the second NBV was selected at $[5°, 160°]$.
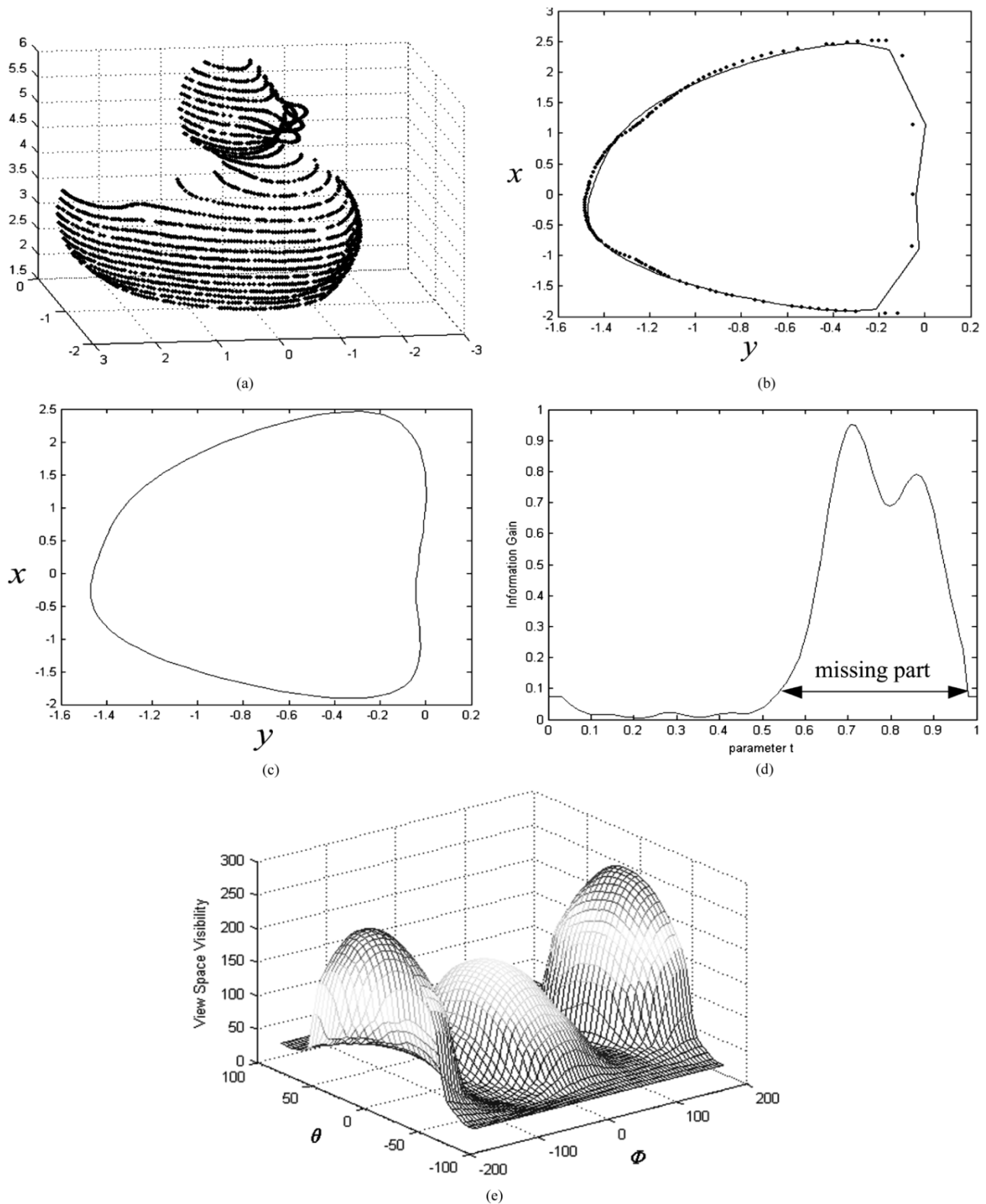
Fig. 12. Reconstruction of cross section curves and predicted information gain. (a) Data acquired from the first viewpoint of the duck model. (b) Data on a cross section acquired from the first viewpoints. (c) Reconstructed B-spline curve. (d) The information gain. (e) "View space visibility" for the first NBV.

The above-described procedures in determining the NBV and acquiring new data are repeated for subsequent next NBVs. The procedures and results in determining the third NBVs are given in Fig. 9. Each time, when new data are available from the new viewpoint, the corresponding cross section curves [e.g., the curve in Fig. 5(b)] are updated [as shown in Figs. 8(c) and 9(b)]. The prediction of the information gain is also updated at each new viewpoint, as seen in Figs. 8(d) and 9(c). As a result of the updated "view space visibility" evaluation at the second NBVs [see Fig. 9(d)], the third NBV was selected at $[7°, -10°]$.

TABLE III
THE RESULTS IN VIEW PLANNING FOR THE DUCK MODEL

Next Best View	1st viewpoint	1st NBV	2nd NBV
Model complexity	7	35	68
Entropy of B-spline	-14.26	-20.23	-30.56

3) Complete Reconstruction: After the third NBV is determined, we obtained the complete data about the object as shown in Fig. 10(a). The complete data points and final reconstruction result of a cross section curve is shown in Fig. 10(b) and (c), respectively.

As shown in Figs. 5(c), 8(d), and 9(c), the information gain has an outstanding peak on the part where the 3-D data are missing. This peak will become less and less outstanding with the increase of the 3-D data available from new viewpoints. When complete data on these cross section curves are obtained (as from the third NBV here), the peak in the information gain becomes nonapparent and appears more "noise, " like [as seen in Fig. 10(d)], which indicates that there are no apparent missing data or occluded parts on the on the object surface. The disappearance of the peak (significant decrease in the peak value) in the information gain was used as the termination condition in automated planning of the NBVs.

From the experiment results, it is observed that the reconstructed model complexity tends to increase with the availability of additional data, which indicates that the model can describe in more and more details about the previously unknown object as new measurements are taken. At the same time, the uncertainty about the object decreases gradually. The results for a typical cross section curve are shown in Table II. The finally reconstructed model is visualized in Fig. 11. The final reconstruction accuracy evaluated using MSE between the actual data points and the reconstructed cross section B-spline curves was 0.0061 which is quite satisfactory.

C. Another Example

Another experiment was also conducted using a model of a duck. For simplicity, we only give the results (in Fig. 12) to show the procedures of determining the first NBV.

The viewpoint $[0°, 175°]$ with maximum information gain was selected as the NBV. The procedures of determining other NBVs are the same as those described in above section. In this example, three viewpoints in total were needed to reconstruct the duck model. The results in view planning for a typical cross section curve are shown in Table III. The accuracy of the finally reconstructed object surface is 0.0076. The reconstructed object is shown in Fig. 13. It is observed that the model complexity for the finally reconstructed cross section curve (68) here is higher than that for the example curve (26) in the previous experiment. This is due to the difference in the shapes from the actual data points. The shape of the former curve [partly given in Fig. 12(b)] is simpler and smoother than the latter [Fig. 10(b)]. A higher complexity in the selected model indicates the higher level of confidence in the reconstruction for a simpler shape. For a complex shape, a lower complexity in the selected model gives it stronger
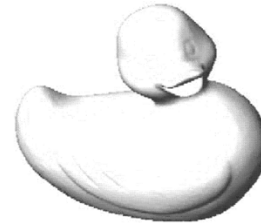

Fig. 13. The finial reconstruction result of the duck model.

ability in preventing over-fitting the data, which is of particular importance for NBV planning.

VI. CONCLUSION

In this paper, we present a novel viewpoint-planning method by incrementally reducing the uncertainties of the reconstructed models. With this method, the object's surface is first decomposed into a set of relative simple cross section curves, with each to be reconstructed by a set of closed B-spline curves. Then the uncertainties of the B-spline models are analyzed with the information entropy as the measurement of the uncertainty for guiding the selection of the NBV. The information gain of the set of cross section B-spline model is predicted and mapped onto the view space. The viewpoint with maximum visibility is selected as the NBV. In addition, an improved BIC criterion is proposed for the model selection. With this new criterion, the acquired data points are divided into two parts: one for estimating the B-spline model parameters and the other for estimating the data noise. The re-sampling of the data enables reliable estimate of noisy data, since the generalization capability of a B-spline model should be validated using another set of data points rather than those used for the approximation. Compared with the conversional BIC criterion, the model selected with our improved BIC criterion is more sensitive to over-fitting and, thus, has better generalization capability, which is particularly important for NBV planning.

REFERENCES

[1] J. Davis and X. Chen, "A laser range scanner designed for minimum calibration complexity," in *Proc. 3rd Int. Conf. 3-D Digital Imaging and Modeling*, ON, Canada, May 2001, pp. 91–98.
[2] Y. F. Li and S. Y. Chen, "Automatic recalibration of an active structured light vision system," *IEEE Trans. Robot. Autom.*, vol. 19, no. 2, pp. 259–268, Apr. 2003.
[3] P. Hebert, "A self-referenced hand-hold ranger sensor," in *Proc. 3rd Int. Conf. on 3-D Digital Imaging and Modeling*, ON, Canada, May 2001, pp. 5–11.
[4] S. Abrams, P. K. Allen, and K. Tarabanis, "Computing camera viewpoints in an active robot work cell," *Int. J. Robot. Res.*, vol. 18, no. 3, pp. 267–288, Mar. 1999.
[5] E. Trucco, M. Umasuthan, A. M. Wallace, and V. Roberto, "Model-based planning of optimal sensor placements for inspection," *IEEE Trans. Robot. Autom.*, vol. 13, no. 2, pp. 182–194, Apr. 1997.
[6] S. Y. Chen and Y. F. Li, "A method of automatic sensor placement for robot vision in inspection tasks," in *Proc. IEEE Int. Conf. Robotics and Automation*, Washington, D.C., May 2002, pp. 2545–2550.
[7] C. I. Connolly, "The determinant of next best views," in *Proc. IEEE Int. Conf. Robotics and Automation*, 1985, pp. 432–435.
[8] J. Maver and R. Bajcsy, "Occlusions as a guide for planning the next view," *IEEE Trans. Pattern Anal. Mach. Intell.*, vol. 15, no. 5, pp. 417–433, May 1993.

[9] R. Pito, "A solution to the next best view problem for automated surface acquisition," *IEEE Trans. Pattern Anal. Mach. Intell.*, vol. 21, no. 10, pp. 1016–1030, Oct. 1999.

[10] P. Whaite and F. P. Ferrie, "Autonomous exploration: Driven by uncertainty," *IEEE Trans. Pattern Anal. Mach. Intell.*, vol. 19, no. 3, pp. 193–205, Mar. 1997.

[11] M. K. Reed and P. K. Allen, "Constraint-based sensor planning for scene modeling," *IEEE Trans. Pattern Anal. Mach. Intell.*, vol. 22, no. 12, pp. 1460–1467, Dec. 2000.

[12] W. Scott *et al.*, "View planning with a registration constraint," in *IEEE Int. Conf. Recent Advances in 3-D Digital Imaging and Modeling*, 2001, pp. 127–134.

[13] S. Fernand and Y. Wang, "Part I: Modeling image curves using invariant 3-D object curve models: A path to 3-D recognition and shape estimation from image contours," *IEEE Trans. Pattern Anal. Mach. Intell.*, vol. 16, no. 1, pp. 1–12, Jan. 1994.

[14] P. Torr, "Bayesian model estimation and selection for epipolar geometry and generic manifold fitting," *Int. J. Comput. Vis.*, vol. 50, no. 1, pp. 35–61, 2002.

[15] P. M. Djuric, "Asymptotic MAP criteria for model selection," *IEEE Trans. Signal Process.*, vol. 46, no. 10, pp. 2726–2734, Oct. 1998.

[16] J. Subrahmonia *et al.*, "Practical reliable Bayesian recognition of 2-D and 3-D objects using implicit polynomials and algebraic invariants," *IEEE Trans. Pattern Anal. Mach. Intell.*, vol. 18, no. 5, pp. 505–519, May 1996.

[17] D. Mackay, "Information based objective functions for active data selection," *Neural Computation*, vol. 4, no. 4, pp. 448–472, 1991.

Y. F. Li (S'91–M'92–SM'01) received the B.S. and M.S. degrees in electrical engineering from Harbin Institute of Technology China. He received the Ph.D. degree in robotics from the University of Oxford, Oxford, U.K., in 1993.

From 1993 to 1995, he was a Postdoctoral Research Associate in the AI and Robotics Research Group in the Department of Computer Science at the University of Wales, Aberystwyth, U.K. He is currently an Associate Professor in the Department of Manufacturing Engineering and Engineering Management at City University of Hong Kong. His research interests include robot vision, 3-D vision, sensing and sensor-based control.
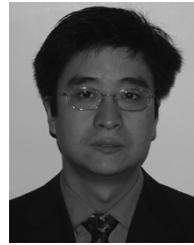
Z. G. Liu received the Ph.D. degree from Xi'an Jiaotong University, Xi'an, China, in 2000.

From then, he joined the National Laboratory of Manufacturing System Engineering, Xi'an Jiaotong University, China. From 2002 to 2003, he worked as a Visiting Researcher at the Department of Manufacturing Engineering and Engineering Management, City University of Hong Kong. He is currently an Associate Professor with the School of Mechanical Engineering of Xi'an Jiaotong University. His research interests include computer vision and 3-D reconstruction.